Valve Dynamics and Internal Waves in a Reciprocating Compressor

by:

Roland Aigner, Georg Meyer and Herbert Steinrück
Institute of Fluid Mechanics and Heat Transfer
Vienna University of Technology
Vienna
Austria
roland.aigner@tuwien.ac.at

4th Conference of the EFRC
June 9th / 10th, 2005, Antwerp

Abstract:

Internal pressure waves influence the performance of reciprocating compressors in two ways: Firstly they interact with the valve dynamics and secondly they excite an oscillating moment onto the piston. On the basis of 2-D and 3-D simulations using a commercial CFD code and the experiences of compressor manufacturers a 1-D flow model is introduced. Valve dynamics are described by a modified Costagliola-model which takes pressure waves in the cylinder into account. Comparison with experiments shows that this 1-D model is sufficient to predict accurately not only gas flow and pressure distribution inside the cylinder but also important design criteria of the valves such as impact velocity of the valve plate and valve losses.

1 Introduction

In the present study we investigate pressure waves in a reciprocating compressor of barrel design. The motivation of this study is twofold. Firstly, during the compression of heavy gases in fast running compressors oscillations of the piston rod have been observed which have been attributed to pressure waves in the cylinder. Secondly, and even more important for the design of compressor valves, it has been observed that the prediction of the impact velocity of the valve plate onto the valve seat is overestimated by conventional methods which do not take the waves in the compressor into account.

At first glance describing the wave systems in a compressor seems to be a complicated task. However, it turns out that a quasi one-dimensional model for the gas flow in the compressor coupled to a simple valve model is sufficient to describe the main effects. Thus an easy to handle design tool based on the above mentioned quasi 1-d model is within reach.

First we review preliminary studies and the state of the art. Then we introduce the quasi 1-d model, compare its solution with a full 2-d, and 3-d solution. But even more important we compare the results with measurements at a test compressor.

1.1 State of the art and preliminary studies

Conventional theories are based on the work done by Costagliola[1]. The change of state inside the cylinder is assumed to be quasi stationary and isentropic. Thus the thermodynamic state (pressure, temperature, density) is taken to be uniform within the cylinder. It is only a function of time. The motion of the valve plate is then determined by the pressure difference across the valve. Since wave phenomena within the cylinder are neglected this leads to considerable deviations of the calculated from the measured valve motion. In particular the impact velocity of the valve plate onto the valve seat differs markedly from measured values.

Studies of E. Machu[2] give a first insight of the effect of waves and unsteady flow inside the cylinder. Simple waves are calculated by the method of characteristics. It is shown that the calculated impact speed is considerably reduced by taking the waves into account. However, the reflections of waves have been neglected and thus the interaction of waves and valve dynamics cannot be described. Moreover this model does not account for geometry effects.

Based on the one dimensional Euler equations G. Machu[3] introduced a model which is capable to describe laterally running waves in the compressor and their interaction with the valve dynamics. This model has been extended by the authors and its results will be compared to full 3d and 2d numerical solutions on the one hand, and more important with measurements on the other hand.

2 Mathematical Model

2.1 Geometry

2.1.1 3-d Simulation

The interior of a reciprocating compressor can be found in figure 1. Valve pockets are located at both sides of the cylinder. The piston is shown in an intermediate position, where it does not mask the valve pockets. The valves are adjacent to the circular lateral surfaces of the valve pockets. Prescribing the motion of the piston and valve boundary conditions, which are described later, this 3-d geometry has been used for a full CFD-simulation. However, computation times which are of the order of several days are too large for every day use.

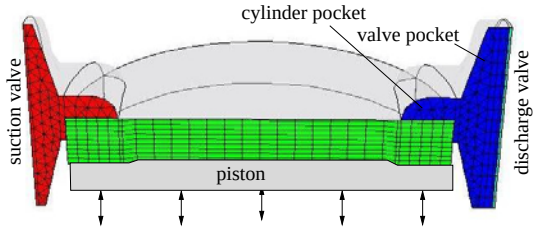

Figure 1: Geometry for 3-d simulation

2.1.2. 2-d Simulation

A remarkable reduction of computation time can be obtained by using a 2-dimensional geometry. However, mapping the original 3-d problem onto a 2-d problem is not trivial at all. Care has to be taken that the volumes and of the 3-d model and the 2-d model are the same. Thus the 2-d domain of computation is a distortion of the cross section of the original geometry. In particular the cylinder is replaced by a cuboid with its length equal to the bore of the cylinder, the same height and same volume. Thus the all length scales in the main direction of the wave propagation and the volumes in the compressor are the same as in the original 3-

d geometry. A detailed description can be found in G. Meyer[5].

2.1.3 1-d simulation

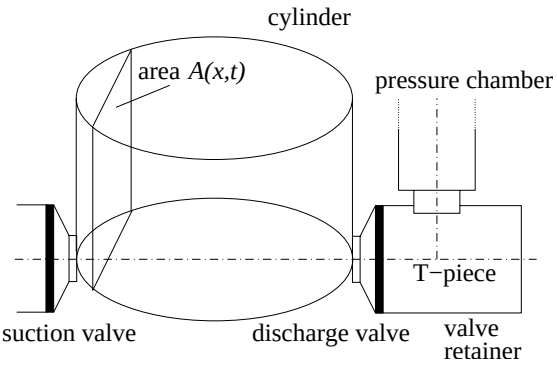

Figure 2: Schema of one dimensional model.

In the quasi 1-d model the wave propagation along the diameter (*x*-axis) of the cylinder from the suction to the pressure valve is considered. The equations of motion (Euler equations) are integrated over a cross section *A(x,t)* perpendicular to the *x*-axis. The effective cross sections of the quasi one-dimensional model are displayed schematically in figure 2. From left to right we have the suction valve, suction valve pocket, cylinder, discharge valve pocket, discharge valve, valve retainer and the pressure chamber, which is connected to the valve retainer by a T-piece.

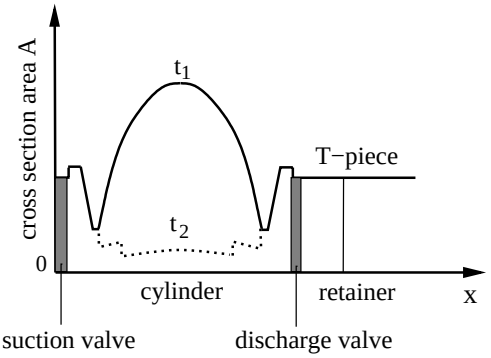

Figure 3: Cross section area A along space coordinate x at time t_1 and time t_2.

Complicated geometries are replaced by simple forms. For instance truncated cones and cylinders represent the valve pockets. If CAD-data of the geometry is available, the cross-section areas along the *x*-axis can be determined directly. Due to the piston motion the cross-section *A(x,t)* inside the cylinder varies with time. Figure 3 shows appropriate area functions depending on *x* at different times t_1 and t_2. At t_2 the piston masks the valve pocket such that the effective cross section area *A(x,t)* is discontinuous there.

2.2 Governing Equations

2.2.1 Piston Motion

The distance between piston and top of cylinder *h* depending on time *t* can be determined using the properties of the crank mechanism. We use the length of the crank lever r, the length of the piston rod l, the smallest distance between piston and cylinder top h_0 an the present angle of the crankshaft φ to obtain

$$h = r + l + h_0 - r\cos\varphi - l\sqrt{1-\left(\frac{r}{l}\right)^2 \sin^2\varphi}\,, \qquad (1)$$

where $\varphi = 2\pi nt$. Here, n denotes the speed of the crankshaft.

2.2.2 Flow Field

The governing equations for the flow of gas are obtained by taking the mass and momentum balance over a cross section. The variables *ρ, u, p* have their usual meaning, density, velocity and pressure, respectively.

$$\frac{\partial \rho A}{\partial t} + \frac{\partial(\rho u A)}{\partial x} = 0\,, \qquad (2)$$

$$\frac{\partial \rho u A}{\partial t} + \frac{\partial(\rho u^2 A + pA)}{\partial x} = p\frac{\partial A}{\partial x}\,. \qquad (3)$$

Assuming isentropic flow conditions we have

$$p\rho^{-\kappa} = \text{const}\,, \qquad (4)$$

where, κ denotes the ratio of specific heats. Note that eq. (3) is not of conservation form. The right hand side of equation (3) constitutes a momentum source of the flow due to a variation of the cross section. Since the cross section *A* may vary rapidly at the transition from the cylinder to the valve pocket, the derivative *dA/dx* may become large causing numerical problems. Using the isentropy condition (4) for smooth solutions the momentum equation becomes

$$\frac{\partial u}{\partial t} + \frac{\partial}{\partial x}\left(\frac{1}{2}u^2 + \frac{\kappa}{\kappa-1}\frac{p}{\rho}\right) = 0 \qquad (5)$$

We remark that equation (5) is equivalent to equation (3) for smooth solutions only. Discontinuous solutions corresponding to shocks or to sudden changes of the flow cross section are associated with an increase of entropy and thus are

not described correctly by (5). However, it turns out that the increase of entropy in the considered cases is small and thus has been neglected.

2.2.3 Valve Dynamics

The state of a valve is specified by the distance between valve plate and seating (valve lift) x_v. The motion of the valve plate is determined by the forces acting on it. We consider the following three contributions to the resulting force: the pressure difference across the valve acting on an effective force area A_v of the valve plate, the springing and thirdly a contribution due to viscous forces in the initial stages of valve opening. Denoting the pressure in front of the valve p_1 and behind the valve p_2 we obtain the equation of motion for the valve plate

$$m_v \ddot{x}_v = (p_1 - p_2) A_v - k(x_v + l_1) - F_{adh}. \qquad (6)$$

Here m_v stands for the mass of the valve plate. The constants k and l_1 denote stiffness of springing and initial deflection of the springs. An initial sticking effect is modelled by the force F_{adh}. It is caused by the viscosity of the gas in the valve gap resulting in a small time delay when the valve is opening. It reads as follows (Flade[4])

$$F_{adh} = f_1 \frac{\dot{x}_v}{x_v^3}. \qquad (7)$$

The factor f_1 depends on geometric features of the valve and properties of the gas. It also takes lubrication oil at the valve plate into account.

2.2.4 Flow through the valve

The flow through the valve is considered as the (stationary) outflow of a gas from a pressurized container through a convergent nozzle. Thus this model takes the pressure loss due to separation into account. The mass flow through the valves is given by St.Venant and Wantzell[6],

$$\dot{m} = \phi \rho_1^0 \left(\frac{p_2}{p_1^0} \right)^{\frac{1}{\kappa}} \sqrt{\frac{2\kappa}{\kappa - 1} \frac{p_1^0}{\rho_1^0} \left(1 - \left(\frac{p_2}{p_1^0} \right)^{\frac{\kappa - 1}{\kappa}} \right)}. \qquad (8)$$

where p_1^0 is the totel pressure before and p_2 is the pressures after the valve, respectively. The effective flow cross section ϕ of the valve is assumed to be a function of the position of the valve plate x_v only. It has to be determined empirically.

2.2.5 T-Piece

It turns out that it is not sufficient to consider pressure waves in the cylinder to describe the valve dynamics. The waves in the valve retainer and pressure chamber have to be taken into account also (see figure 2). In the quasi 1-d model it is described by two pipes connected at a junction or T-piece. We require that a junction itself has no volume and that the mass and energy balances are satisfied.

3 Numerical Solution

3.1 Finite Volume Method

For the numerical analysis it is useful to write the continuity equation (2) and the equation of motion (5) in conservation form:

$$\frac{\partial \mathbf{u}}{\partial t} + \frac{\partial \mathbf{f}(\mathbf{u}, x)}{\partial x} = 0, \qquad (9)$$

where the state vector $\mathbf{u} = (\rho A, u)^T$. and $f(u,x)$ is the so called flux function.

The computational domain consists of the interior of the compressor, including the cylinder and the valve pockets, the valve retainer and the pressure chamber. The equations of motion (9) are solved by a finite volume scheme. Since the cross section of the flow domain is not constant special care has to be taken. The f-wave algorithm by LeVeque[4] can handle even discontinuous cross sections of the flow domain.

3.2 Boundary and Interface Conditions

The finite volume scheme has to be supplied with appropriate boundary conditions. If the valves are closed, they are described as a fixed wall, by setting $u=0$. If the valve is open the mass flow is prescribed. It is obtained by equation (8) as a function of the total pressures before and after the valve and the valve plate position. The pressure outside the suction valve is kept constant. To determine the pressure after the discharge valve wave propagation in the valve retainer and the pressure chamber is computed using the finite volume scheme. At the end of the pressure chamber

the pressure is prescribed. The equation of motion (6) of the valve plate is solved simultaneously by an explicit second order scheme.

3.3 Time step

The time step Δt of the numerical integration has to be chosen such that the stability conditions of the numerical schemes are satisfied. On one hand the CFL condition $\Delta t<\Delta x/(c+|u|)$, where Δx is the interval length of the spatial discretization and c is the velocity of sound and on the other hand $\Delta t < m_v/k$ have to hold.

4 Comparison of the numerical solutions with measured data

4.1 Experimental setup

A double acting, 2 cylinders, barrel design reciprocating compressor was tested at Burckhardt Compression, Switzerland. The main specifications of the compressor can be found in table 1.

Type of compressor	Burckhardt Compression 2K90-1A: 2 cylinders, double acting
Bore diameter	0.22 m
Stroke	0.09 m
Speed of Crankshaft	980 ÷ 990 rpm
Clearance	1.5 mm
Type of valve	110K12
Gas	Air
Ambient pressure	0.97 bar
Discharge pressure	1 ÷ 5 bar

Table 1: Main specifications of the experimental compressor.

Pressure sensors inside the cylinder and valve retainer (see figure 4) record the pressure at different locations.

In order to ensure a fair comparison of measured data with numerical simulations three of four working chambers have been sealed off during measurements by covering the valve pockets of these chambers.

The relative pressures in the diagrams are referred to an ambient pressure of 0.97 bar (at the day of measurements).

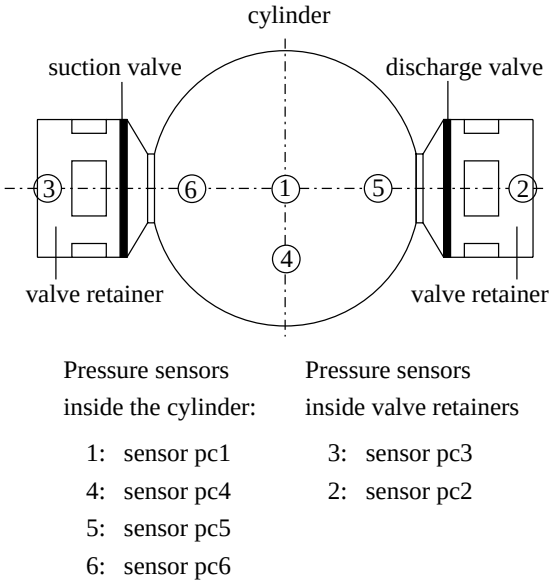

Figure 4: Position of pressure sensors

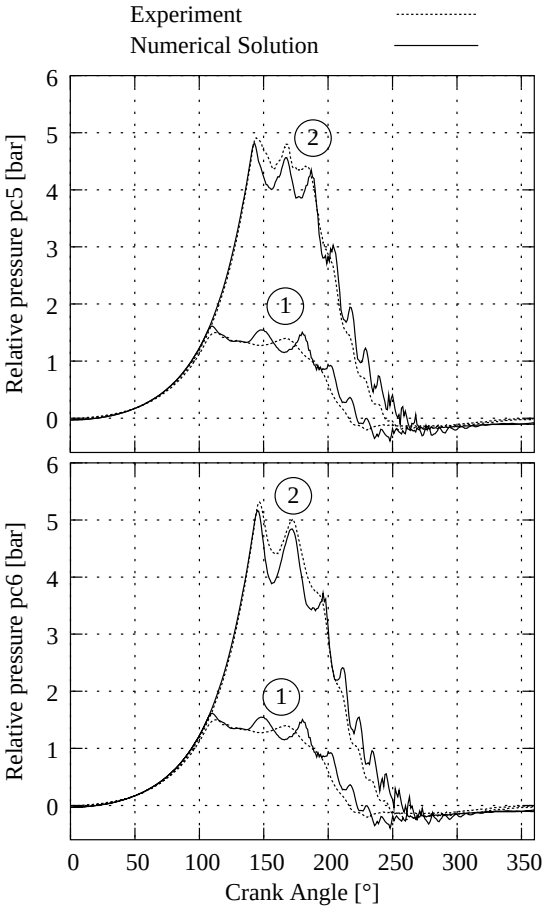

Figure 5: Comparison of numerical solution of quasi 1-d model and experiment, a) pressure at discharge valve, b) pressure at suction valve for discharge pressures of 2 bar (curves 1) and 5 bar (curves 2)

In figure 5 a comparison of the measured pressures at pc5 and pc6 with the numerical solution of the quasi one dimensional model for discharge

pressures of 5 bar and 2 bar are given. In figure 6 a comparison of the pressure at pc2 in the valve retainer is given. In the following we will discuss the solutions in detail. Here and in the following we will focus on the case with discharge pressure 5 bar only.

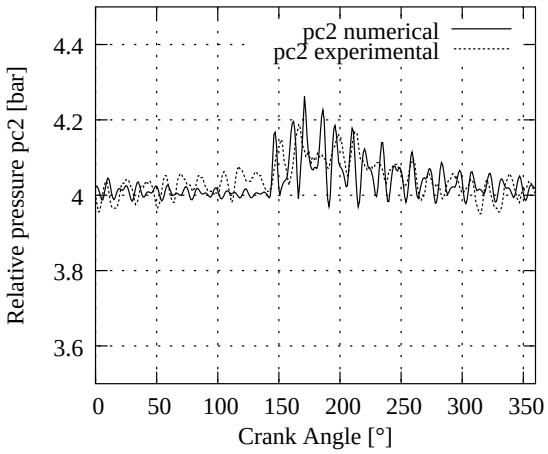

Figure 6: Pressure in the valve retainer at pc2.

4.2 Initiation of waves

In figure 7 the pressure readings at pc5 and pc6 close to the discharge valve and the suction valve, respectively, and the position of the valve plate as a function of the crank angle are shown.

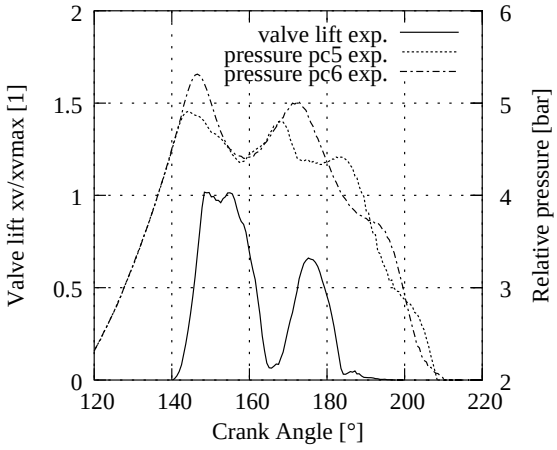

Figure 7: Initiation of waves by the opening of the discharge valve: pressure close to discharge valve dotted line, pressure at suction valve dashed line, position of valve plate solid line

The pressure distribution inside the compressor is shown in figure 8. During compression when both valves are closed the pressure is uniform in the cylinder (CA=140°). When the pressure in the cylinder exceeds the pressure in the valve retainer plus the springing the valve starts to open. The pressure near the outflow valve ceases to increase and reaches a maximum, while the pressure close to the suction valve still increases. The opening of the valve has initiated a wave which reaches the opposite side of the cylinder at a crank angle CA=146°, just before the valve has completely opened. Then the rarefaction wave is reflected at the suction side. Thus the pressure at pc6 attains also a maximum. But it is markedly larger than that on the pressure side (sensor pc5).

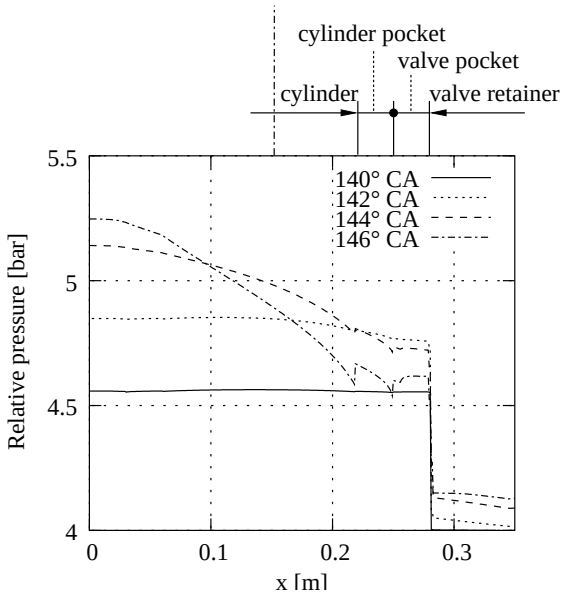

Figure 8: Pressure distribution in the cylinder and valve retainer at wave initiation CA=140° discharge valve still, closed, CA=142° valve opens, at suction side still isentropic compression, CA=146° rarefaction wave has reached suction side.

When the valve plate hits the valve seat the pressure in front of the pressure valve is large enough to keep the valve open until CA=155°. Then the pressure has dropped such that the valve begins to close again reducing the mass outflow. This tends to increase the pressure again. The increase of pressure forces the valve to open and a complicated interaction of the valve motion with the pressure waves in the cylinder takes place. Shortly after the piston has passed the lowest volume dead centre the valve closes finally. At that time a complicated system of waves travelling back and forth is left in the cylinder. In figure 9 the difference of the pressure readings at pc5 and pc1 is shown and compared with the numerical solution. We observe that during expansion the waves are damped and their period tends to the travelling time of waves across the cylinder, *2d/c,* corresponding to the lowest eigen mode in lateral direction. We want to point out that at the beginning of the expansion phase a mix of modes with several eigen frequencies have been present.

These modes have been all initiated by the valve motion. As said above the zeroth eigen mode has the smallest damping and remains visible until the suction phase starts.

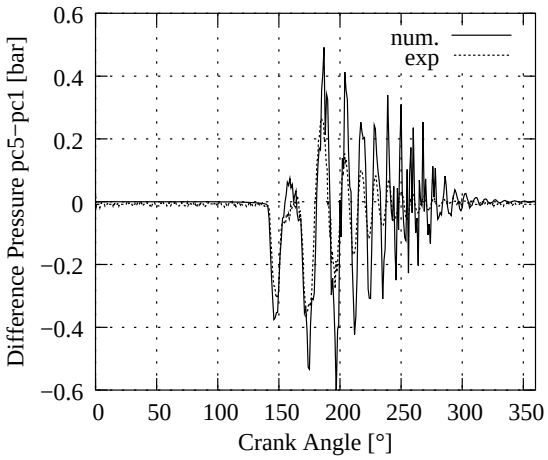

Figure 9: Difference of pressures at discharge valve and cylinder centre (pc5-pc1)

4.3 Super elevation of the pressure due to initial sticking

Comparing the pressure reading pc5 close to the discharge valve with the corresponding numerical solution shows that opening of the valve is predicted to early (see figure 10).

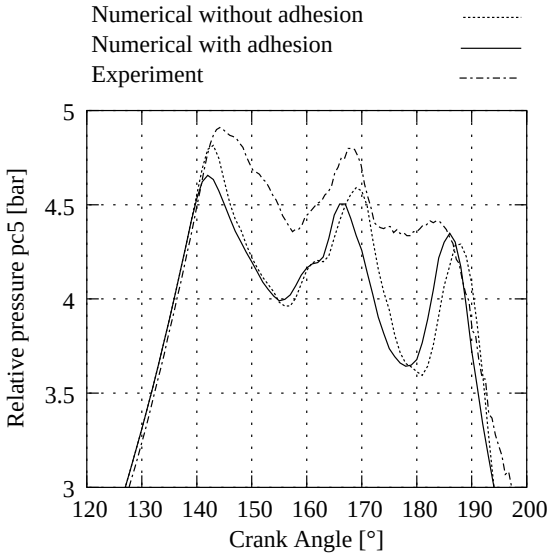

Figure 10: Delay of valve opening due to viscosity in valve gap

As a consequence the pressure maximum at pc5 is about 0.2 bar to small. With other words in reality the opening of the valve does not start when the pressure in the cylinder balances the pressure in the retainer and the springing. An additional delay occurs. In Flade[4] the dynamic behaviour of a valve plate is analyzed. If the initial gap is very small, say in the range from 1μm to 5μm viscosity hinders the gas to flow into the valve gap resulting in a local pressure drop in the valve gap. Applying asymptotic methods an additional force holding back the valve plate can be identified (7). It turns out that the result depends on the initial gap width, which cannot be measured easily. Here the initial gap width 1.5μm has been chosen to fit the data.

4.4 Pressure loss at sudden change of cross section.

In Figure 11 the pressure at pc5 computed with the method where the pressure loss is taken into account is compared with the measurements and the numerical solution without this correction.

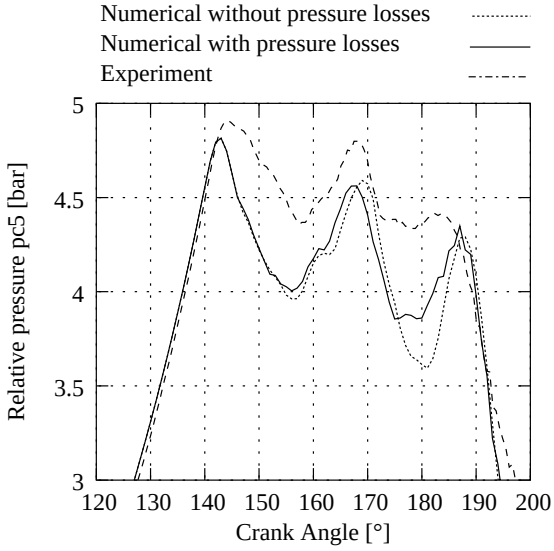

Figure 11 Effect of pressure loss at entrance to cylinder pocket: Solution without pressure loss (dotted line), with pressure loss (solid line) and measure data (dashed line)

The pressure at pc5 predicted by the numerical solution where the sticking effect has not been taken into account drops after the first maximum at an crank angle of 144° to a minimum at CA 156°. This minimum is about 0.4 bar smaller than that of the measured data. At the second minimum at a crank angle of 180 degrees (dead centre) the difference is even worse (0.8 bar). A possible explanation for this difference may be the following. During outflow the gas is compressed under the piston. There it flows through a narrow channel towards the valve pocket. At the entrance of the cylinder pocket the gas faces a sudden increase of the effective cross section of the flow channel. This sudden increase of the cross section is physically associated with a pressure loss which

is not accounted for in the present model. We impose at the sudden change of cross section continuity of the mass flow and pressure. This procedure is applied only if the discharge valve is open and the ratio of effective cross section after and before is larger than an arbitrary value, say 3. Otherwise equation (5) is used.

The deviation of the simulation from the measurement is decreased, but still considerable. It is believed that the flow at the entrance of the cylinder pocket is two- or three dimensional.

4.5 Influence of the waves in the retainer

Considering the motion of the valve plate we observe that the first opening of the discharge valve agrees more or less with the measured data. But there are remarkable differences in the second opening. The numerical solution predicts that the valve opens again completely, but measurements show that is opens only to 65%. This is attributed to the fact that waves are neglected in the valve retainer. Taking the valve retainer and its connection to the pressure chamber modelled as a T-piece into account good agreement for the valve motion is obtained (see figure 12).

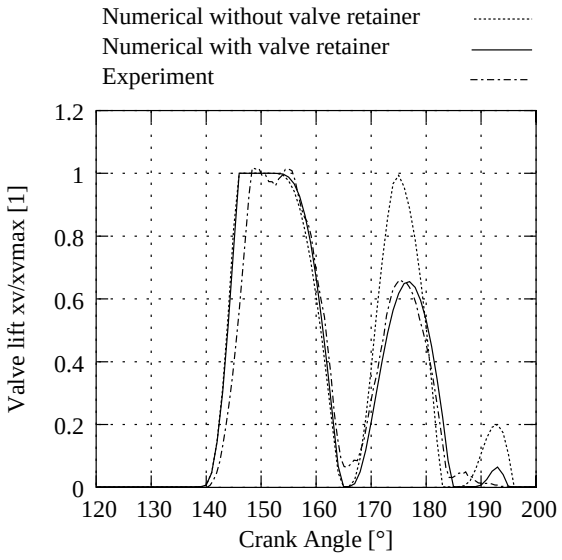

Figure 12: Influence of pressure waves in the valve retainer

4.6 Damping of waves during expansion

In figure 13 the difference between the pressures at the discharge valve and the centre of the cylinder pc5-pc1 as a function of the crank angle is shown after the discharge valve is closed. This pressure difference represents the waves in the cylinder.

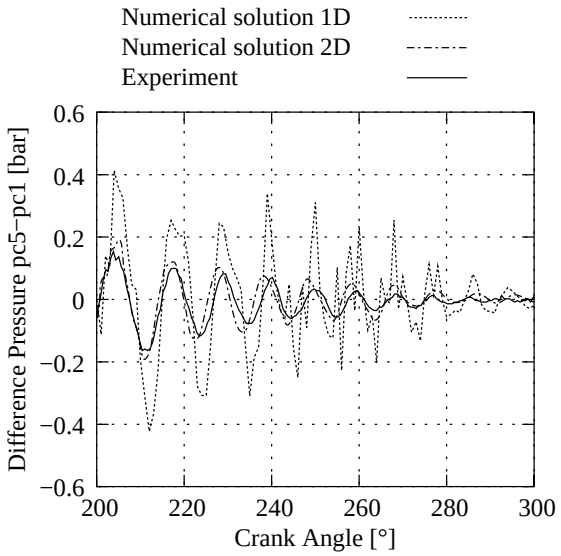

Figure 13: Damping of the waves during expansion: Numerical solution of 1-d model compared with numerical solution of 2-d model and measured data

During expansion the waves in the compressor are damped. The numerical solution of the quasi 1-d model, the numerical solution of a 2-d model and the measured date are compared. The damping rate of the solution of the 2-d model agrees well with the observed one. The damping predicted by the quasi one-dimensional is slightly too small.

The excitation of waves is overestimated by the 1-d model resulting large amplitudes. It has to be noted that the numerical solution of the 2-d dimensional model has been obtained for a relatively fine grid. 3198 cells in the upper dead centre and 15978 cells at the lower dead centre. For coarser grids the damping phase has been dominated by numeric dissipation giving unrealistic strong damping. However, 3d simulation using a sufficient fine grid to resolve the damping of the waves would take a couple of weeks and thus has not been performed. The high numerical dissipation of the used Solver FLUENT 6.1.22 is caused by the first order accuracy of time integration when using dynamic meshing. There is hope that using a second order time integration coarser meshes can used such that a 3d-simulation becomes reasonable.

4.8 The impact velocity

The impact velocity of the valve plate onto the valve seat can be extracted form the valve motion. In figure 14 the calculated and measured impact velocities for different discharge pressures are compared and are in good agreement.

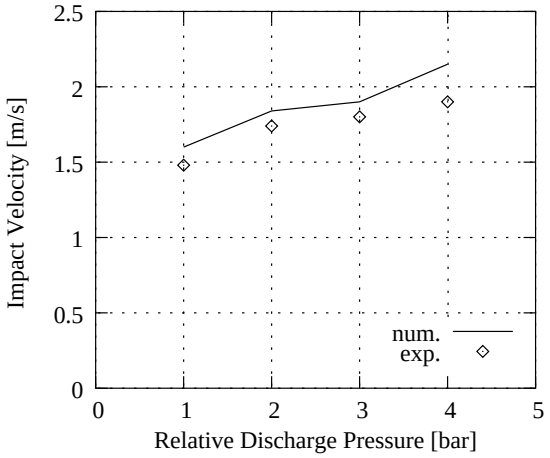

Figure 14: Impact velocities

4.9 Valve losses

In figure 15 the computed mean pressure *p* is shown in the p,V-diagram. The shaded area corresponds to losses at the discharge valve.

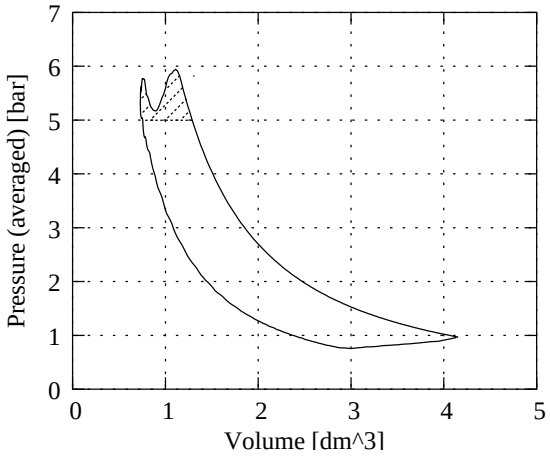

Figure 15: p,V-diagram, valve losses

5 Comparison with 2-d and 3-d CFD simulations

To verify the assumptions of the quasi 1-d model CFD simulations using FLUENT 6.2 β-release have been performed. The valve dynamics are implemented by user defined functions. The mass flow through the valve is calculated using the St. Vernant Wanzell formula (8) and is distributed evenly as mass sinks (or sources) over the first cell row adjacent to the valves. A detailed description can be found in G. Meyer[5].

Here we show the pressure distribution at the cylinder cap (figure 16a) and in the (vertical) plane of symmetry of a compressor (figure 16b). Near the centre line the curvature of the pressure surfaces is small. Thus we expect that the internal flow is well approximated by the quasi 1-d model. The interaction between the valve dynamics and the waves in the compressor turns out to be similar. The advantages of the CFD simulation are that regions where the flow is two or three dimensional are well represented, for instance the flow in the valve pockets. The main disadvantage is the large computation time which is due to the fine mesh needed to resolve the waves properly. Otherwise the waves are unrealistically damped by numerical dissipation.

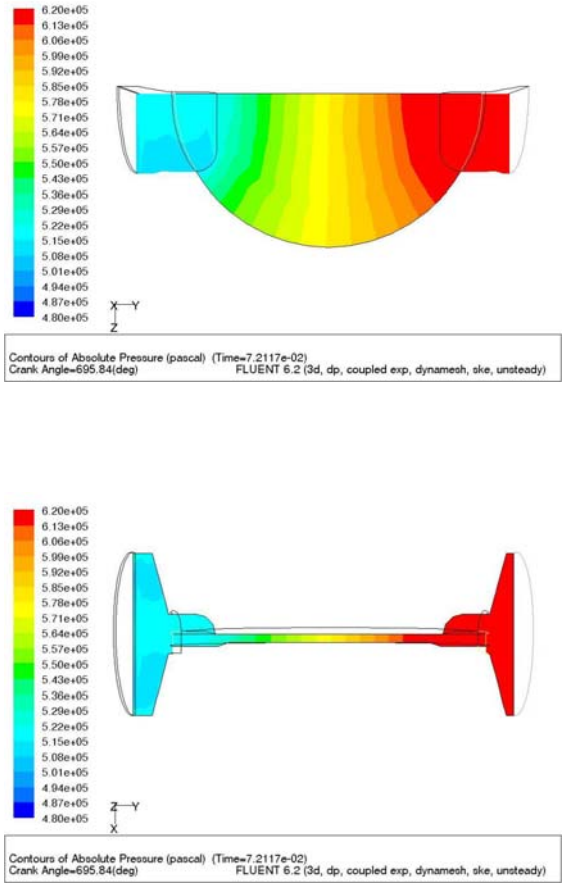

Figure 16. Pressure distribution at the cylinder cap (a) and in the symmetry plane (result of 3d simulation)

6 Conclusion

In the project 'The flow in a reciprocating compressor' sponsored by the EFRC different models predicting the pressure waves in the cylinder and their interaction with the valve dynamics are investigated. Following an idea of G.Machu[3] it turns out that a quasi 1-d model is sufficient. In particular the impact velocity of the valve plate onto the valve seat can predicted well.

Thus the quasi 1-d model will be used as the basis of design tool.

Future research will include the investigation of fast running compressor for heavy gases. The moment onto the piston will be of special interest and how it can be influenced by a special shape of the piston.

In a parallel project the heat transfer from the cylinder wall and piston rod onto the gas will be investigated.

7 Acknowledgements

The research is financand by the European Forum for Reciprocating Compressors. The authors want to thank G. Machu and P. Steinrück (Hoerbiger) and G. Samland and D. Sauter (Burckhardt Compression) for many fruitful discussions.

References

[1] Costagliola, M. (1950): The Theory for Spring Loaded Valves for Reciprocating Compressors. J. Appl. Mech, 415-420.

[2] Machu, E. (1998): Problems with modern high speed short stroke reciprocating compressors: Increased power requirement due to pocket losses, piston masking and gas inertia, eccentric gas load on the piston. Gas machinery conference USA

[3] Machu, G. (2004): Calculating reliable impact valve velocity by mapping instantaneous flow in a reciprocating compressor. Gas machinery conference USA

[4] Flade, G., Steinrück, H. (2004): Anfängliches Öffnungsverhalten von Kompressorventilen. PAMM Proceedings in Applied Mathematics and Mechanics, 4, 450-451.

[5] Meyer, G. (2004): Simulation der Strömung in einem Kolbenverdichter. Diplomarbeit, TU-Wien

[6] Zierep, J. (1997): Grundzüge der Strömungslehre. Springer Berlin Heidelberg.